ELSEVIER

Earth and Planetary Science Letters 192 (2001) 407–421

EPSL

www.elsevier.com/locate/epsl

Rifted(?) crust at the East Antarctic Craton margin: gravity and magnetic interpretation along a traverse across the Wilkes Subglacial Basin region

Fausto Ferraccioli [a,*], Franco Coren [b], Emanuele Bozzo [a], Claudio Zanolla [b], Stefano Gandolfi [c], Ignazio Tabacco [d], Massimo Frezzotti [e]

[a] *Dipartimento per lo Studio del Territorio e delle sue Risorse (DIPTERIS), Università di Genova, Corso Europa 26, 16132 Genoa, Italy*

[b] *Istituto Nazionale di Oceanografia e di Geofisica Sperimentale, Trieste, Italy*

[c] *DISTART, Università di Bologna, Bologna, Italy*

[d] *Dipartimento Scienze Terra, Università di Milano, Milan, Italy*

[e] *ENEA, Rome, Italy*

Received 30 January 2001; received in revised form 18 April 2001; accepted 26 July 2001

Abstract

Early geophysical studies hypothesized a continental rift structure beneath the Wilkes Subglacial Basin. Recent models favour a flexural origin for the basin linked to Transantarctic Mountains uplift and to East Antarctic Craton lithospheric rigidity. Flexural modelling predicts crustal thickening beneath the basin. Gravity modelling along the International Trans-Antarctic Scientific Expedition traverse (1998/99), however, reveals crustal thinning beneath the basin. At 75°S the crust thins from 37 km beneath the Transantarctic Mountains to 31 ± 2 km beneath the Wilkes Basin. The western flank of the basin features a sharp magnetic break. This signature may arise from a fault separating highly magnetic Precambrian craton crust from weakly magnetic Neoproterozoic(?) crust. Much later crustal extension may have focussed along the craton margin. The eastern flank of the Wilkes Basin exhibits a prominent aeromagnetic signature. Potential field modelling predicts 1–4 km thick sedimentary infill within the Wilkes extended terrane, interpreted mainly as Beacon Supergroup intruded by Jurassic Ferrar tholeiites. The adjacent Adventure Subglacial Trench is a narrow rift basin with 25 ± 5 km thick crust and a 10 ± 4 km sedimentary infill.

Keywords: geophysical surveys; Transantarctic Mountains; riftzones crust; Ferrar Group; tholeiite; East Antarctica

1. Introduction

East Antarctica is thought to feature thick, stable and coherent Precambrian continental lithosphere [1]. In contrast, the West Antarctic Rift lithosphere compares to major Cenozoic continental rift systems [2–4]. The crustal structure of

* Corresponding author. Tel.: +39-10-353-8091; Fax: +39-10-353-8091.

E-mail address: magne@dipteris.unige.it (F. Ferraccioli).

0012-821X/01/$ – see front matter
PII: S0012-821X(01)00459-9

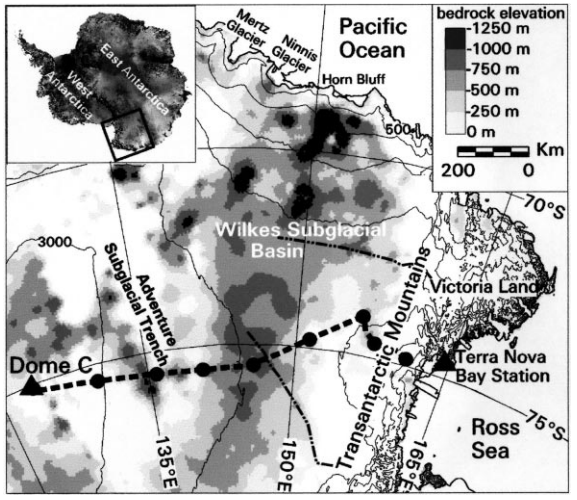

Fig. 1. Location of the ITASE traverse (heavy dash) across the Wilkes Subglacial Basin region over the BEDMAP bedrock compilation [15]. Circles are fuel depots and repeat magnetic and gravity stations. Light dashes show previous geophysical traverses [16,17].

the Transantarctic Mountains, forming the West Antarctic Rift shoulder, has been studied with gravity [5,6], aeromagnetic [7] and large offset seismic data [8]. The poorly known Wilkes Subglacial Basin lies in the remote and entirely ice-covered hinterland of the range (Figs. 1 and 2). It is a 1250 km long subglacial feature detected by reconnaissance airborne radio-echo sounding [9]. Mean bedrock elevation is about 500 m b.s.l. from George V Coast, where the basin is about 400 km wide, to latitude 81°S, where it is about 100 km wide [10]. The deeper (1000 m b.s.l.) and narrower Adventure Subglacial Trench lies along the western flank of the Wilkes Basin [10]. Early radar, aeromagnetic, gravity and seismic investigations are not located along coincident profiles over the region. The geophysical dataset was first interpreted to indicate that the region could represent rifted continental crust with a sedimentary infill of about 3 km [9,11]. Stern and ten Brink [12] proposed instead a flexural origin for the Wilkes Basin in 45 km thick cratonic crust. This hypothesis depicts the basin as an 'outer low' linked to Transantarctic Mountains uplift and to the high flexural rigidity of the East Antarctic Craton lithosphere [13]. Seismic reflection, radar, magnetic and gravity data were acquired during the EAST-93 traverse to test the validity of the flexural model [14]. Modelling along EAST-93 appears to confirm the validity of the flexural hypothesis and newly incorporates the effects of Cenozoic transtension between East and West Antarctica [14]. This traverse at 78°S did not, however, cross the entire width of the basin.

Aiming to investigate the controversial crustal structure of the Wilkes Subglacial Basin, we present results of an oversnow gravity and magnetic traverse combined with airborne radar data crossing the entire width of the basin at about 75°S. This dataset was acquired by an Italian party within the ITASE (International Trans-Antarctic Scientific Expedition) in the 1998/99 field season.

2. Geological and geophysical background

2.1. Basement

The 500 Ma Ross Orogen forms the basement of Victoria Land [18]. Model ages indicate buried Precambrian crustal components [19]. Since Precambrian units outcrop along George V Coast and Terre Adélie Coast [20] they might occur beneath the Wilkes Basin (inset in Fig. 2). The unexposed boundary between the East Antarctic Craton and the Ross Orogen may lie at 155°E between George V and Oates coasts (Fig. 2) [21]. Long-wavelength aeromagnetic anomalies could reveal buried high-grade Precambrian shield rocks west of the Central Victoria Land Boundary (CVLB) [22]. Alternatively, these anomalies may reveal Ross Orogen magmatic arc rocks along a buried thrust fault zone [7]. Fig. 2 shows a new model suggesting that the CVLB may lie along the easternmost edge of the Wilkes Basin. Therefore the more recent interpretation [7], if correct, shifts the location of unreworked Precambrian basement further to the west, possibly beneath the Wilkes Basin.

2.2. Beacon and Ferrar rocks

Denudation of the Ross Orogen formed the

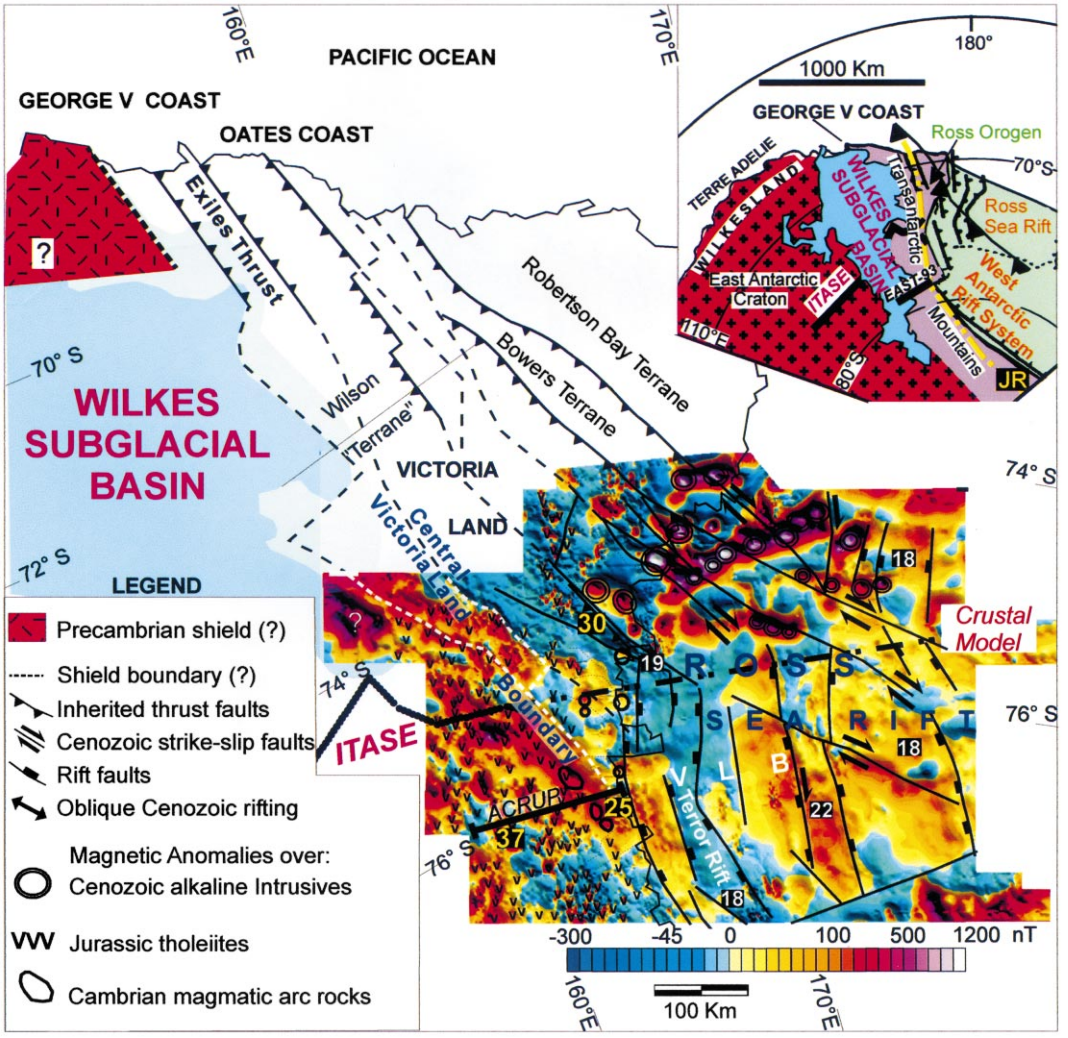

Fig. 2. Tectonic sketch, aeromagnetic map and seismic crustal thickness estimates in km (black boxes) over the Transantarctic Mountains–Ross Sea Rift [7] adjacent to the Wilkes Subglacial Basin study area. Pale and dark blue shade over the basin is 250 and 500 m b.s.l. respectively [10]. The inset shows subduction beneath the East Antarctic Craton forming the Ross Orogen, the inferred Jurassic tholeiitic rift (JR), the West Antarctic Rift and the ITASE and EAST-93 across the Wilkes Basin. Note the locations of the ACRUP seismic line and of the Ross Sea Rift extension of our crustal model. VLB, Victoria Land Basin.

Silurian to Early Devonian Kukri Peneplain. The overlying Devonian to Jurassic Beacon Supergroup was deposited in intracratonic or in foreland basins parallel to the palaeo-Pacific margin [23,24]. Ferrar Group (Kirkpatrick Basalt and Ferrar Dolerite) tholeiites were emplaced at 184 ± 1 Ma [25]. Jurassic dikes and faults indicate pre- and syn-Ferrar crustal extension related to early Gondwana break-up [26]. Present exposure of Ferrar rocks suggests a narrow and elongate magmatic belt, the Jurassic Transantarctic rift [26,27]. Magnetic anomalies trace these tholeiites beneath ice cover [7] and gravity data reveal buried Beacon Supergroup [14]. Therefore these rocks, if present, might be detected remotely in the hinterland of the Transantarctic Mountains.

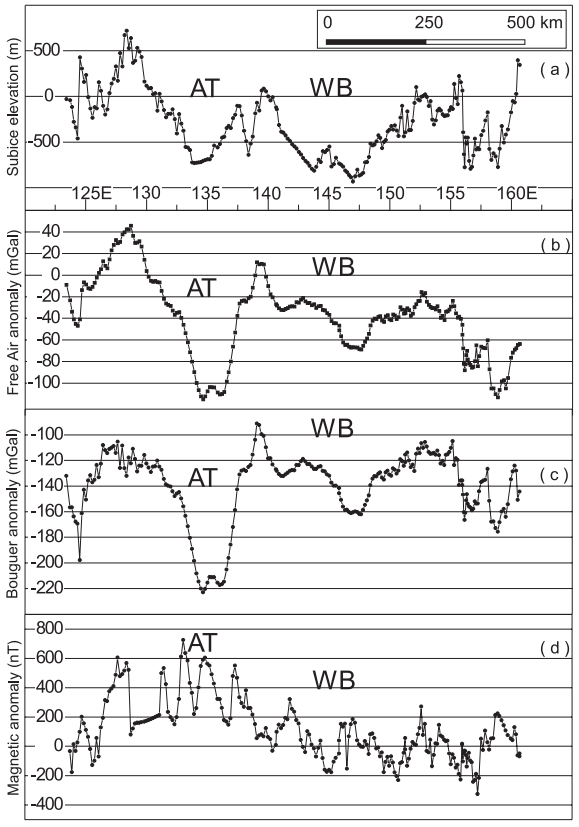

Fig. 3. Traverse profile data include: (a) subice bedrock elevations; (b) free air gravity anomalies; (c) Bouguer anomalies; (d) magnetic anomalies. WB, Wilkes Subglacial Basin; AT, Adventure Subglacial Trench.

2.3. Ross Sea rifting and Transantarctic Mountains

Crustal thickness is 30–37 km over Victoria Land [8] (Fig. 2). Ross Sea rift basins lie parallel to the Transantarctic Mountains and to the Wilkes Basin and feature highly extended, less than 20 km thick crust, with up to 14 km of sediments [3]. Cretaceous rifting was coeval with Gondwana break-up in the Pacific Ocean [28]. Substantial Transantarctic Mountains uplift is coeval with Eocene-to-present(?) rifting and alkaline magmatism [28]. This rifting phase may relate to reactivation of Ross age faults in a right-lateral strike-slip kinematic regime and to Australia–Antarctica transform faulting [29]. Oblique Cenozoic rifting [30] is consistent with aeromagnetic patterns [22,7]. Post-Jurassic offset across the West Antarctic Rift–Transantarctic Mountains margin is estimated to be 3000 m and the age of the oldest drilled rift sediment is 34 Myr [31]. Sirius Group marine diatoms of the Transantarctic Mountains could indicate marine sedimentation in the Wilkes Basin region during periods of minimum East Antarctic ice sheet volume in the Neogene [32]. These marine diatoms could, however, be wind-blown rather than transported by the East Antarctic ice sheet and might therefore not require the presence of Pliocene seas in the Wilkes Basin [33].

3. ITASE traverse and geophysical datasets

Within the ITASE traverse from Terra Nova Bay Station to Dome C about 230 gravity and magnetic stations supplemented by airborne radar were acquired (Fig. 1). Potential field station were 5 km apart and were positioned using differential GPS with an accuracy of ± 5 m.

3.1. Airborne radar dataset

The airborne ice-penetrating radar survey was performed at 300 m above the ice surface. Folded dipole radar antennas were deployed under each wing. The rover GPS was synchronised with the master GPS station at Terra Nova for differential correction. The ground-sampling rate was 5–6 m. A constant EM wave propagation velocity of 168 m/μs was assumed for the East Antarctic Ice Sheet. Root mean square (rms) error in ice thickness is ± 8 m. The resulting bedrock surface is shown in Fig. 3a.

→

Fig. 4. Map view renderings across the Wilkes Basin region compiled with data from the adjacent Transantarctic Mountains [5–7] including: (a) bedrock topography [10]; (b) free air anomaly grid; (c) Bouguer anomaly grid; (d) magnetic anomaly grid. Bold black lines are major anomaly breaks. Contours of bedrock topography in all panels.

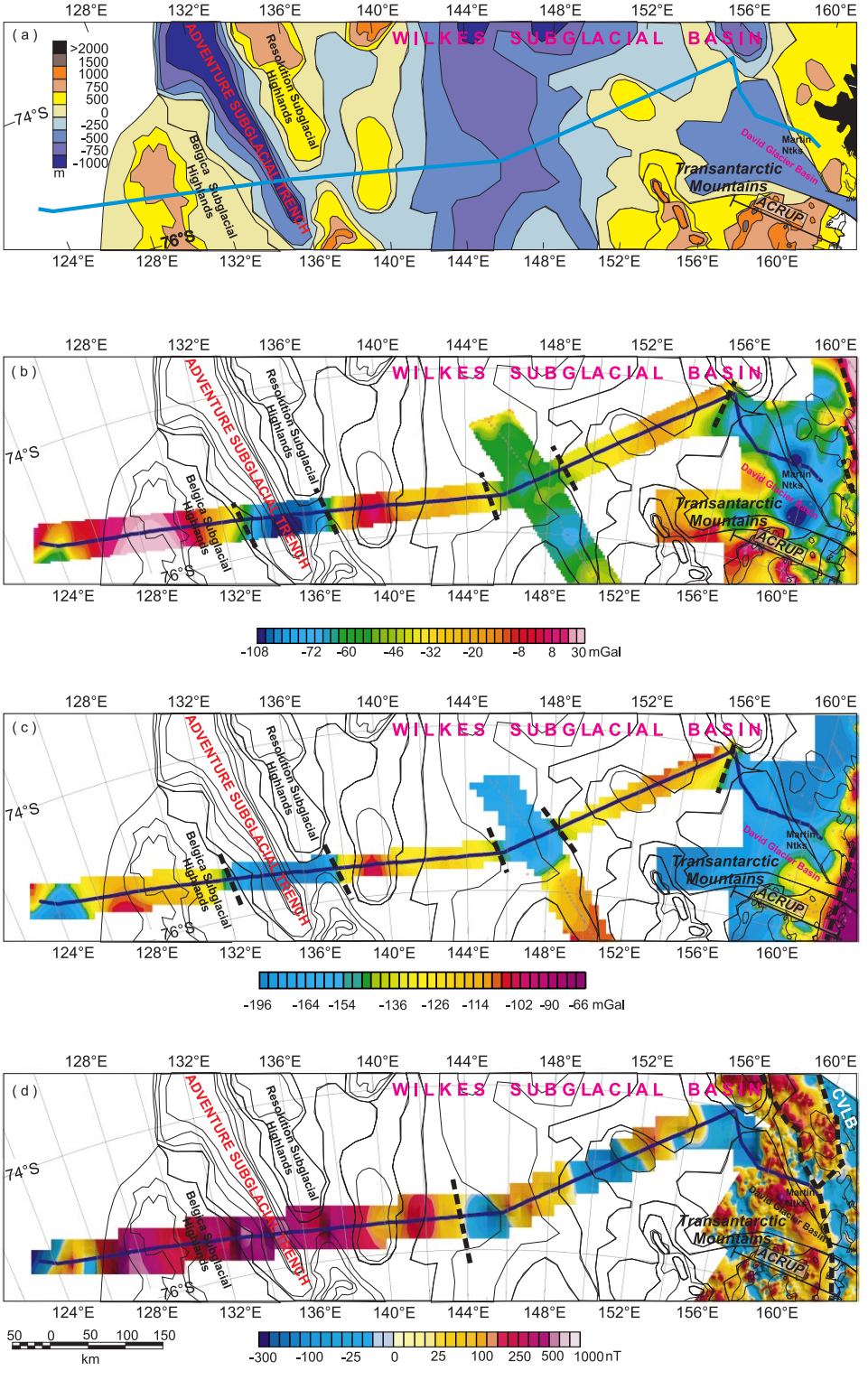
(a)
(b)
(c)
(d)
WILKES SUBGLACIAL BASIN
ADVENTURE SUBGLACIAL TRENCH
Resolution Subglacial Highlands
Belgica Subglacial Highlands
Transantarctic Mountains
ACRUP
Marin Ntks
David Glacier Basin
CVLB
128°E 132°E 136°E 140°E 144°E 148°E 152°E 156°E 160°E
124°E 128°E 132°E 136°E 140°E 144°E 148°E 152°E 156°E 160°E
74°S
76°S
>2000 1500 1000 750 500 0 -250 -500 -750 -1000 m
-108 -72 -60 -46 -32 -20 -8 8 30 mGal
-196 -164 -154 -136 -126 -114 -102 -90 -66 mGal
-300 -100 -25 0 25 100 250 500 1000 nT
50 0 50 100 150 km

3.2. Gravity dataset

A LaCoste and Romberg gravimeter was adopted. Processing involved quality control, instrumental drift and measurement compensation, and the removal of tide effects. The gravity profile was tied to the absolute gravity station at Terra Nova Bay [34]. Gravity anomalies were calculated using the Geodetic Reference System Formula of 1967. The GPS elevation was corrected for geoid undulation using the OSU91 model. The free air anomaly was computed (Fig. 3b). The Bouguer anomaly (Fig. 3c) was calculated with density reference values of 2.67 kg/cm^3 for rock and $\rho = 0.9$ kg/cm^3 for ice. A rugged bedrock topography and a poor control on 3-D ice thickness variations precluded accurate computations of corresponding gravity corrections. Hence data accuracy is about ± 5 mGal.

3.3. Magnetic dataset

Two Scintrex proton precession magnetometers were used. One operated as the base station and the other as the rover station. Data processing involved quality control, base station correction and IGRF removal. Low-pass filtered data from Terra Nova Bay, Scott Base and Dome C obser-

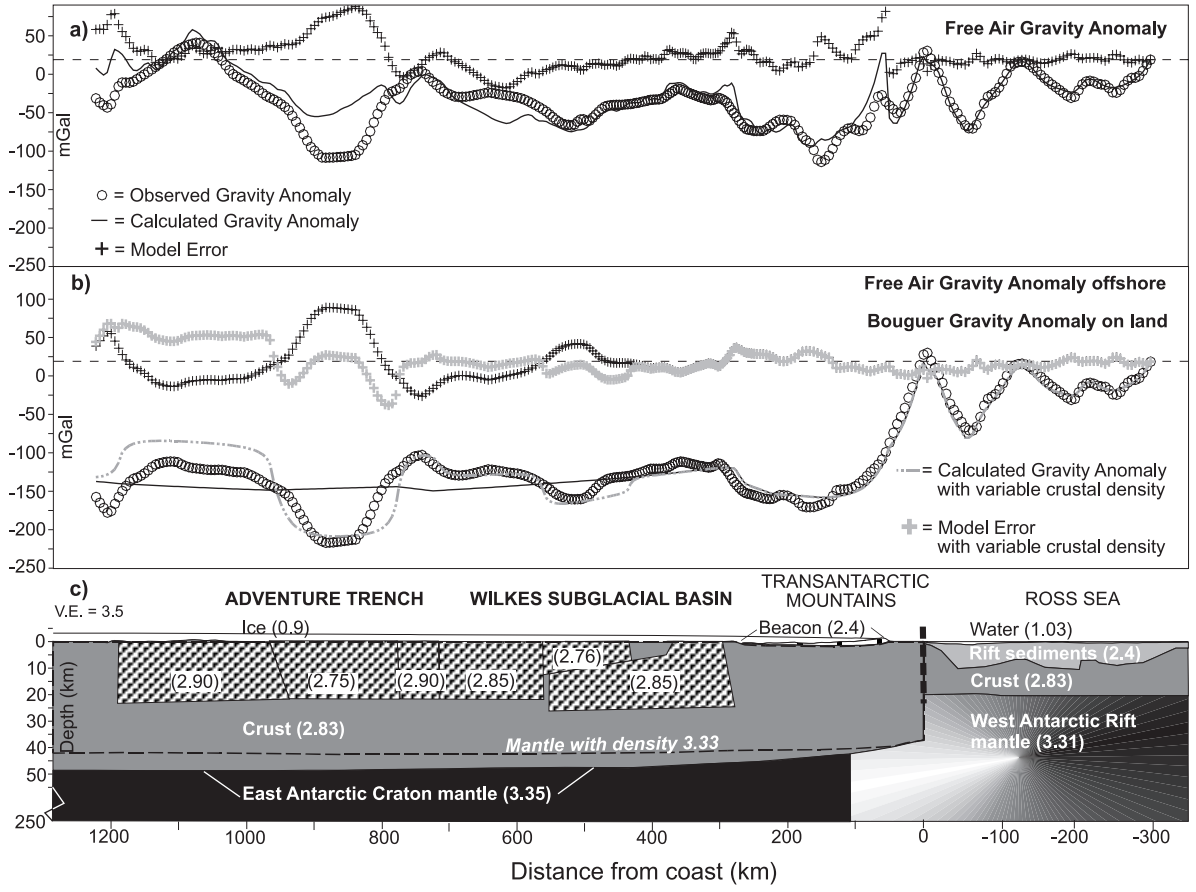

Fig. 5. Flexural gravity modelling of the Wilkes Basin. (a) Observed vs. calculated free air anomaly field and the model error. (b) Observed vs. calculated free air anomaly (offshore) and Bouguer anomaly field (onshore) and the model error. The gravity model response obtained by introducing bodies with variable crustal density is also shown. Note in panel c the contrasting upper mantle model densities (g/cm^3) of the West Antarctic Rift and East Antarctic Craton and crustal thickening beneath the Wilkes Basin region.

vatories were used to reduce magnetic time variations. Diurnally corrected repeat stations (Fig. 1) suggest poor accuracy for the magnetic anomaly data (±40 nT) owing to high-amplitude external field variations. The data are nevertheless sufficiently precise to assess regional magnetic pattern (Fig. 3d).

4. Potential field anomalies

The ITASE dataset was first integrated with previous potential field data over the Transantarctic Mountains [5–7] and bedrock topography mapping [10] to obtain an improved picture of regional structure (Fig. 4a–d). The N–S Wilkes Subglacial Basin is a 300 km wide, asymmetrical, subglacial trough (Figs. 3a and 4a). There is an elevation difference between the rough basin floor and its shoulders of about 1000 m. The NNW Adventure Subglacial Trench is a narrower, about 50 km wide basin, 750–1000 m b.s.l. A negative free air anomaly of −60 mGal marks the centre of the Wilkes Basin (Figs. 3b and 4b). The basin flanks exhibit instead relatively positive anomalies. A sharp Bouguer anomaly break occurs at 156°E at the eastern flank of the basin (Figs. 3c and 4c). This step separates the negative Bouguer anomaly field of the Transantarctic Mountains (−200 to −180 mGal) from the broad high over the basin (−140 to −120 mGal). A relative Bouguer low in the axial part of the basin is well defined at 148°E (−40 mGal). A more prominent negative anomaly marks the Adventure Subglacial Trench (−100 mGal). High-frequency magnetic anomalies with amplitudes between +200 and −200 nT mark both the Wilkes Basin and the adjacent Transantarctic Mountains (Figs. 3d and 4d). A sharp magnetic break occurs at 144°E along the western margin of the Wilkes Basin. To the west of the Wilkes Basin magnetic anomalies have longer wavelengths and higher amplitudes (up to +700 nT).

5. Crustal modelling

Two-dimensional forward and inverse gravity and magnetic modelling was performed across the Wilkes Subglacial Basin, the Transantarctic Mountains and adjacent Ross Sea Rift (Figs. 5–8). In this way the responses of the flexural hypothesis [12–14] and of the rift hypothesis [9–11] were tested along the ITASE traverse across the Wilkes Subglacial Basin region (Fig. 5 vs. Fig. 6). The strike of the modelled structures was assumed to be normal to the model profile. The location of the model extension across the Ross Sea Rift is displayed in Fig. 2. The offshore part of the gravity models is fairly well constrained because of the availability of independent seismic constraints over the Ross Sea. The −100 mGal free air gravity anomaly over the Victoria Land Basin is modelled with the seismic proxy of an 18–20 km deep Moho and 10–14 km thick sedimentary rift infill [3,5] leading to a rms model error of 3 mGal. Onshore independent wide-angle seismic modelling results are available for the Transantarctic Mountains along the ACRUP line at 76°S [8], i.e. 100 km south of the ITASE traverse.

Flexural uplift of the Transantarctic Mountains along the Ross Sea Rift flank may have generated the broad downwarped Wilkes Basin if the East Antarctic Craton lithosphere is highly rigid [12]. Stern and ten Brink [12] modelled old gravity data [17] as being consistent with the flexural hypothesis. However, these data had a high degree of uncertainty both in elevation and in ice thickness (as much as 100 m). We found a 30 mGal misfit at the intersection between previous traverse data and the ITASE data. Isostatic equilibrium between East and West Antarctica has been assumed in flexural models to reduce the non-uniqueness of predicted structures and placed at a 200 [12] or 250 [14] km compensation depth. A density contrast between the lithospheric mantle of East Antarctica and West Antarctica was introduced to maintain the isostatic equilibrium. This density contrast would be consistent with significant variation in lithospheric rigidity, implying strongly contrasting geotherms in the two diverse Antarctic provinces [12–14]. The thermal imbalance associated with this upper mantle difference also supplies an important driving force for Transantarctic Mountains uplift [12]. The presence of low-density mantle beneath the Victo-

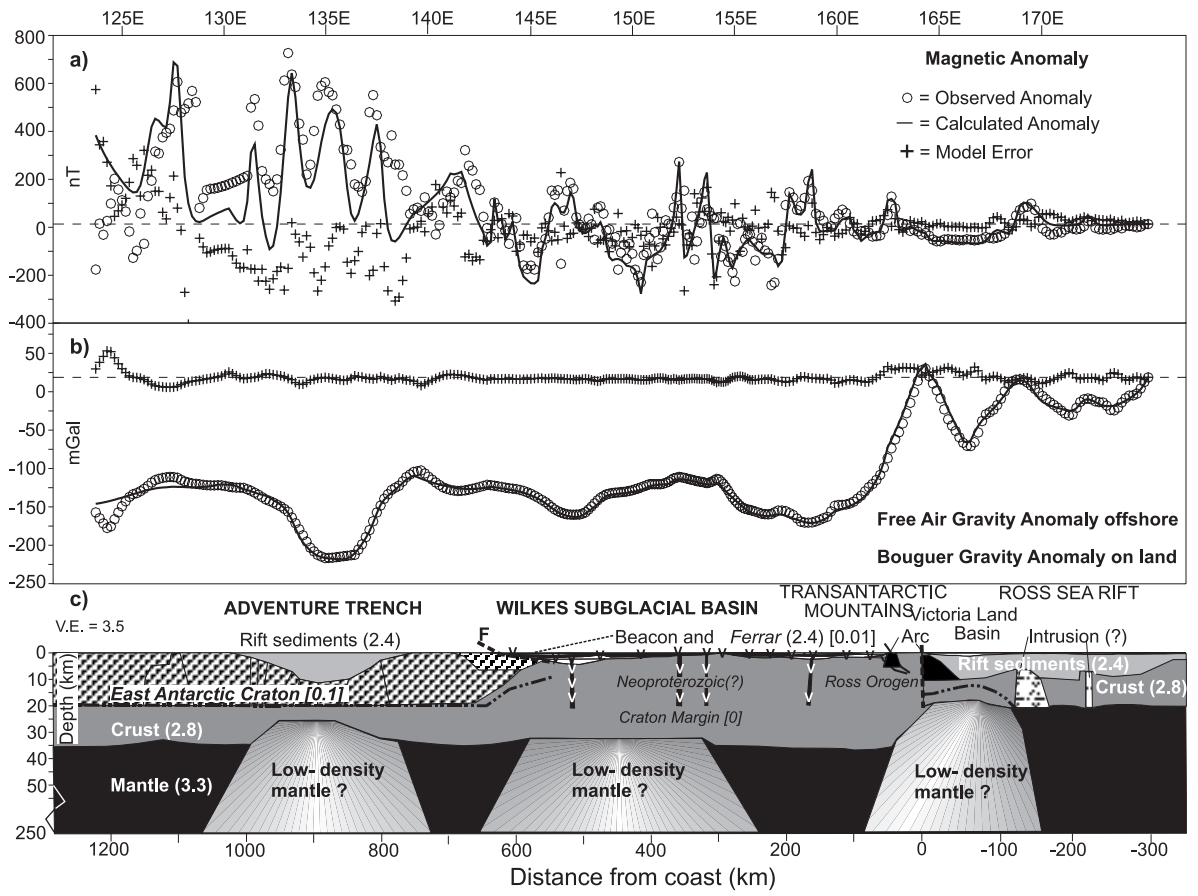

Fig. 6. Rift gravity model of the Wilkes Basin region. (a) Observed vs. calculated magnetic anomaly and the model error. (b) Observed vs. calculated free air anomaly (offshore) and Bouguer anomaly field (onshore) and the model error. Note in panel c modelled crustal thinning beneath the Wilkes Basin and Adventure Trench and the sedimentary infill. Square brackets are apparent magnetic susceptibilities in SI units. Dashed line shows possible upwarp of the Curie isotherm beneath the Wilkes Basin.

ria Land Basin would indeed explain the anomalously low upper mantle seismic velocities [3]. In analogy to previous models in our flexural gravity model we therefore introduced an East Antarctic Craton mantle with a 3.35 g/cm^3 density and a hotter West Antarctic Rift mantle extending 100 km beneath the uplifted Transantarctic Mountains with a 3.31 density (Fig. 5a–c). The overlying crust was assigned a constant 2.83 g/cm^3 density, while Ross Sea Rift and Beacon sediments were given a 2.4 g/cm^3 value. In this model configuration the crust thickens from about 20 km beneath the Ross Sea Rift to 45 km beneath the Transantarctic Mountains in good agreement with previous flexural model estimates further south [12]. The crust would flex downward to about 47–48 km beneath the Wilkes Basin region. The misfit between observed and calculated anomalies is relatively small over the Transantarctic Mountains (rms 10 mGal). The rms error increases to 20 mGal in the Wilkes Basin and is over 40 mGal over the Adventure Trench. Also the broad calculated Bouguer low differs from the observed lows over the basins which exhibit well-defined flanking highs. Moreover, ACRUP seismic models [8] indicate that the crust beneath the Transantarctic Mountains is 37 km rather than 45 km thick. A flexural model with a 37 km crustal thickness beneath the range requires less density and hence less thermal contrast between

East and West Antarctic upper mantle (dashed line in Fig. 5c). However, even if this were the case the gravity misfit over the hinterland basins is not reduced. The model error over the basins diminishes only if a variable upper crustal density is introduced in the East Antarctic Craton crust. Overall a simple flexural model does not appear to fit the observed data over the Wilkes Subglacial Basin region.

A simple rift model is more consistent with the observed gravity anomalies since it leads to a rms error of 5 mGal over the subglacial basins and a 4 mGal overall error (Fig. 6a–c). The regional Bouguer high over the Wilkes Basin can be modelled as a broad 300 km wide mantle upwarp and associated broad crustal thinning. Contrary to previous flexural models to the south [14] the Beacon(?) sedimentary layer can be modelled to continue in the Wilkes Basin itself. The high-frequency magnetic anomalies over the basin, which resemble those over the adjacent Transantarctic Mountains [7], might reflect Ferrar(?) dolerite sills intruding the Beacon strata. Apparent susceptibility (mean = 0.01 SI) and thickness of the modelled Beacon–Ferrar(?) layer is likely to be variable. Thickness of this inferred 'sedimentary' layer was found to vary between 1 and 4 km, possibly reflecting structural highs and lows [11]. Magnetic basement was not required beneath the 'sedimentary' layer in the Wilkes Basin. To the west of the basin, thick magnetic crustal basement with a variable but high mean apparent susceptibility (0.1 SI) is required. This magnetic basement may reveal extensive East Antarctic Craton crust, as discussed later. The Adventure Trench negative gravity anomaly is modelled by introducing a 100–150 km wide rift basin with about 10 km sedimentary infill overlying thin crust. Low-density mantle might be possible beneath the modelled rift structures but is not required to fit the gravity data.

The inherent problem with the flexural and our preferred rift gravity model is the lack of independent constraints on depth and geometry of the sediment/crust and crust/mantle interfaces over the Wilkes Basin region. We therefore assessed possible error bounds on crust and sediment thickness in the rift gravity model by studying the effect of varying sediment/crust/mantle density contrasts beneath the basins. For example, if crustal thickness beneath the Adventure Rift Basin(?) is assumed to be 25 km (models AT1–3), then sediment thickness may vary from 14 to 10 km as its density decreases from 2.4 to 2.3 g/cm^3 (Fig. 7b and Table 1). If one assumes that the sedimentary layer is 10 km thick, then the crust could be 27 km thick or 29 km thick for sediment densities of 2.35 and 2.4 g/cm^3 respectively (AT6–5 in Fig. 7c). A low-density upper mantle beneath the rift (3.28 g/cm^3) would lead to a model with 21 km thick crust and a 13 km sediment infill, or a model with 25 km thick crust and 10 km thick sediment (AT8–9). Overall the

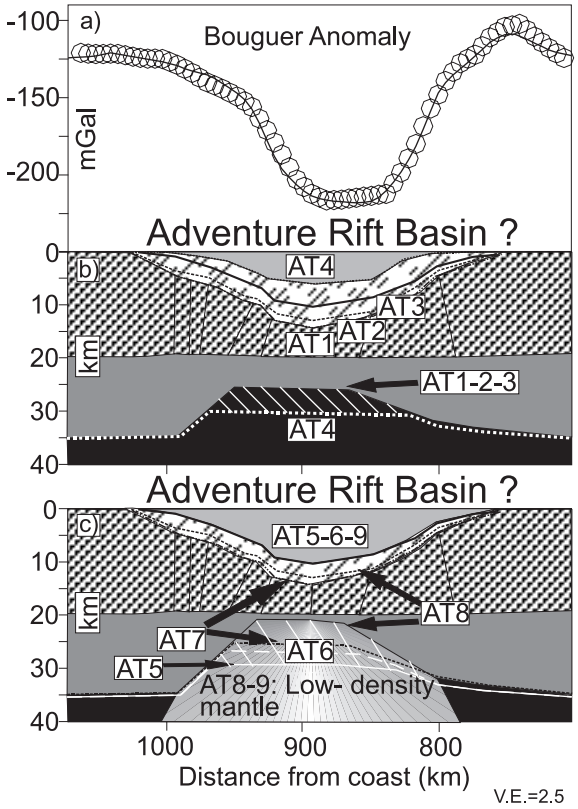

Fig. 7. (a) Observed Bouguer anomaly (circles). The calculated gravity anomaly response (solid line) over the interpreted 'Adventure Rift Basin?' is identical for models AT1–4 (b) and AT5–9 (c). Black diagonal hatch is estimated sediment thickness error envelope. Opposite directed diagonal hatch (white) is the estimated Moho depth error envelope. See Table 1 and text for details.

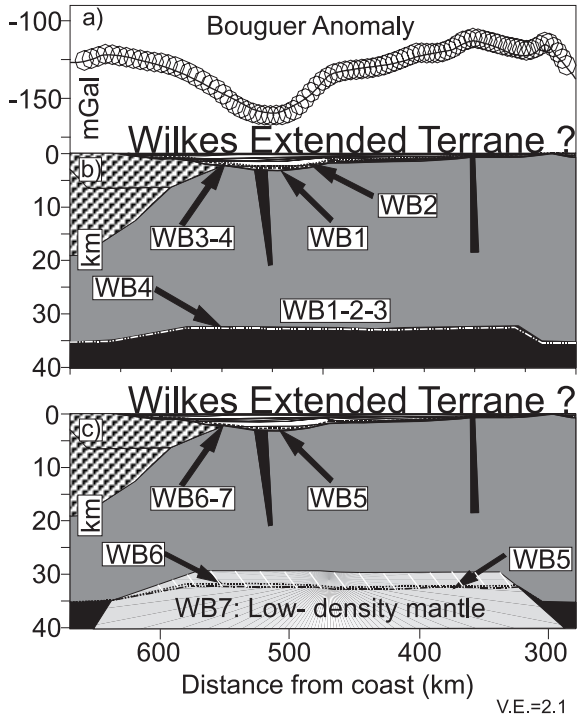

Fig. 8. (a) Observed Bouguer anomaly (circles). The calculated anomaly response over the interpreted 'Wilkes Extended Terrane?' is identical for models WB1–4 (b) and WB5–7 (c). Note the Moho depth error envelope displayed as in Fig. 7b,c. Maximum sediment thickness is 3–4 km. See Table 1 and text for details.

Adventure Rift crust can be estimated to be 25 ± 5 km thick, while the sedimentary infill is 10 ± 4 km thick. Similar model calculations were performed for the Wilkes Basin representing a possible broad region of extension (WB1–7 in Fig. 8a–c), leading to a 31 ± 2 km thick crust and a maximum sediment thickness of 3–4 km (Table 1). To further constrain crustal structure of the Wilkes Subglacial Basin, modelling results are combined with the results from independent regional studies in Fig. 9. The complementary geophysical results we considered include: Moho estimates from the spectral correlation analysis of Antarctic gravity and terrain data [35]; Antarctic Magsat crustal anomalies at 400 km altitude [36]; crustal thickness estimates along the ACRUP seismic and gravity profile [6,8]; and aeromagnetic interpretation over the adjacent Transantarctic Mountains [7].

6. Extended(?) crust in the Wilkes Subglacial Basin region

Our rift model (Fig. 6a–c) indicates crustal thinning beneath the Wilkes Subglacial Basin region rather than crustal thickening predicted by flexural models [12]. The concept that East Antarctic crust is uniformly over 40 km thick would nevertheless be consistent with early surface-wave dispersion studies [37]. The widely distributed seismic propagation paths may, however, have led to averaging across the Antarctic, resulting in an overestimate of the crustal thickness for the Wilkes Basin region.

Our crustal modelling predicts 31 ± 2 km thick crust for the Wilkes Basin in basic agreement with a recent Moho map for the Antarctic continent [35]. This map, derived from spectral correlation of observed free air gravity anomalies and calculated terrain gravity effects, indicates 28–34 km thick crust for the Wilkes Basin (Fig. 9). The crust is therefore thinner relative to the Transantarctic Mountains, which exhibit values between 34 and 47 km [35]. In the Wilkes Basin region, however, only limited surface gravity observations were available for constructing the Moho map, so low-degree satellite-derived geopotential models and the Air–Heiskanen topographic–isostatic po-

Table 1
Effect of varying choices of sediment/crust/mantle densities (g/cm^3) on crust and sediment thickness (km) estimates beneath the Adventure Trench and Wilkes Basin

Model	Densities	Crust	Sediment
AT1	2.4/2.8/3.3	25	14
AT2	2.35/2.8/3.3	25	13
AT3	2.3/2.8/3.3	25	10
AT4	2.2/2.8/3.3	30	6
AT5	2.4/2.8/3.3	29	10
AT6	2.35/2.8/3.3	27	10
AT7	2.35/2.85/3.3	25	14
AT8	2.35/2.8/3.28	21	13
AT9	2.35/2.8/3.28	25	10
WB1	2.4/2.8/3.3	32	4
WB2	2.35/2.8/3.3	32	3.5
WB3	2.3/2.8/3.3	32	3
WB4	2.4/2.8/3.3	33	3
WB5	2.35/2.8/3.3	31.5	3.5
WB6	2.3/2.8/3.3	31	4
WB7	2.4/2.8/3.28	29	4

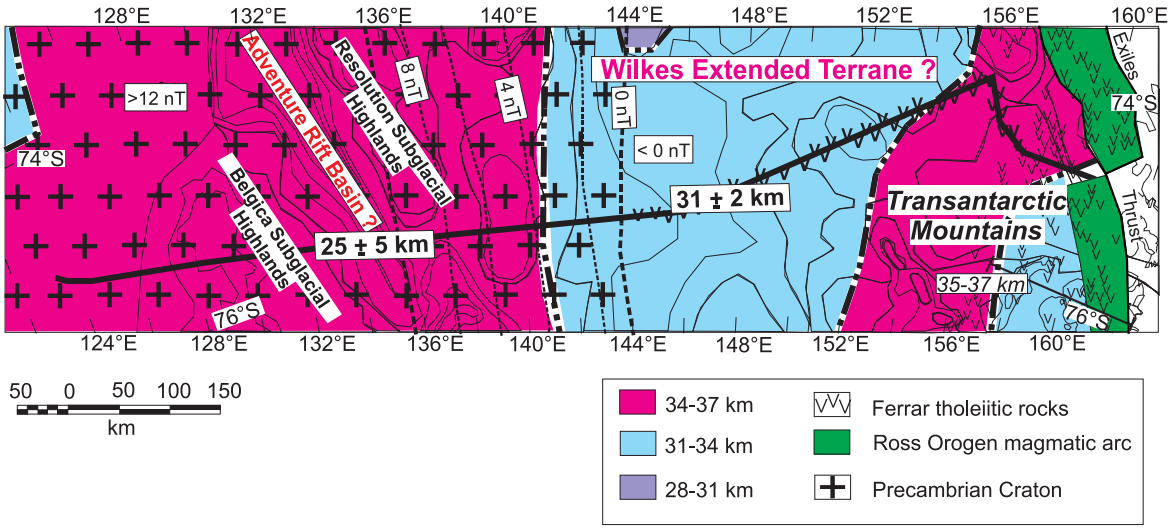

Fig. 9. Interpretation map of the Wilkes Subglacial Basin region suggesting thinned continental crust for a wide region of the 'Wilkes Extended Terrane?' and for the narrow region of the 'Adventure Rift Basin?'. Crustal thickness estimates (bold values) along ITASE are compared to colour-coded estimates between heavy dashed contours derived from a previous Antarctic Moho map and the ACRUP seismic estimates (italicised values). Dashed contours of Magsat anomaly values highlight the magnetic break along the western flank of the Wilkes Basin at the inferred margin of the craton. Large V symbols along the traverse are used to indicate a possible much wider Ferrar Province than previously inferred from aeromagnetic data (small V) over the adjacent Transantarctic Mountains.

tential were adopted [35]. The distinct Moho upwarp we modelled over the 'Adventure Rift Basin' is not imaged in the Antarctic Moho map. The −100 mGal gravity anomaly over the 'Adventure Rift Basin' is similar to the −100 mGal Victoria Land Basin anomaly in the Ross Sea Rift. The 'Adventure Rift Basin' anomaly also resembles the Kenya Rift gravity anomaly (figure 5.2 in [4]). The 'Adventure Rift Basin' does not appear to feature a negative magnetic anomaly comparable to the one observed over the Terror Rift (Fig. 2). Given the considerable sediment thickness beneath the Adventure Trench, the lack of comparable rift signature may reflect highly magnetic crustal basement flooring and surrounding the basin or comparatively lower heat flow. The Wilkes Subglacial Basin features a regional magnetic low. Speculatively the broad magnetic low over the basin might reflect high heat flow and associated upwarp of the Curie isotherm induced by broad crustal extension (Fig. 6c).

The broad Wilkes Subglacial Basin, modelled to feature relatively thin sedimentary infill and small lateral gradients in crustal thickness, could speculatively involve an 'extended crustal terrane' reminiscent of the broad Basin and Range Province. The narrower and deeper Adventure Subglacial Trench, with modelled thick sedimentary infill and larger lateral crustal thickness gradients, is more reminiscent of narrow modern rift basins such as the Kenya rift or the Baikal rift [4]. Our hypothesis that continental crust in the Wilkes Subglacial Basin region may involve modern extended crust is in agreement with the hypothesis of Steed [11]. Large-throw half-grabens interpreted from radio-echo sounding along the western flank of the Wilkes Basin [11] would be consistent with our gravity model for the inferred 'Adventure Rift Basin'. Multi-channel seismic data collected offshore George V Coast also suggest recent faulting (Brancolini, personal communication, 2001). Post-Jurassic faulting of Beacon–Ferrar layers along the eastern flank of the Wilkes Basin, interpreted from radar data [9,11], would match the aeromagnetic fault interpretation at the western edge of the Transantarctic Mountains [7]. In addition, continental overlap in Late Cretaceous Australia–Antarctica seafloor reconstruc-

tions may be reconciled with continental extension in the Wilkes Basin region [38].

Our extensional hypothesis for the Wilkes Basin region at 75°S is hard to reconcile with the flexural hypothesis along the EAST-93 at 78°S [14]. This may imply either that the Wilkes Basin region is extensional in origin in the north but flexural in the south or that the EAST-93 traverse does not extend far enough west over the Wilkes Basin to detect rift-related gravity signatures. Aerogeophysical surveys over the Wilkes Basin would be needed to further test extensional models vs. previous flexural models. Wide-angle and seismic reflection experiments are also required to better constrain crust and sediment thickness. Seismological and deep electrical conductivity studies could constrain thermal and rheological parameters.

7. Precambrian craton bounded by the western flank of the Wilkes Subglacial Basin

Highly magnetic crust results to the west of the Wilkes Subglacial Basin in contrast to weakly magnetic crust to the east. Analysis of US–Italian aeromagnetic data over the Wilkes Basin confirms the presence of this major magnetic break (Bell, personal communication, 2001). A linear break along the western flank of the Wilkes Subglacial Basin is imaged in Antarctic Magsat [36] and in POGO [39] data. The western flank of the Wilkes Subglacial Basin corresponds to the eastern margin of the high-amplitude Wilkes Land positive satellite anomaly (Fig. 9). In contrast the Wilkes Subglacial Basin features a broad negative satellite anomaly [36,39]. Correlation between the geology of the formerly contiguous Gawler Craton in southeastern Australia and the East Antarctic Craton is generally recognised (e.g. [20]). The elevated magnetic signature of Wilkes Land may reflect Precambrian lithosphere of the East Antarctic Craton in analogy to the high-amplitude anomaly over the Gawler Craton [39]. The negative magnetic anomaly over the Wilkes Subglacial Basin resembles the negative magnetic anomaly [40] over the Neoproterozoic Adelaide Fold belt at the eastern margin of the Gawler Craton [41]. Precambrian rock types including amphibolites, granulitic mafic gneisses and orthogneisses with susceptibilities almost as high as the apparent susceptibilities introduced in the crustal model have been measured west of Ninnis Glacier [42] (Fig. 2). A basement fault zone along the western flank of the Wilkes Subglacial Basin (F in Fig. 6c) may separate dominantly high-grade craton-type crust to the west from younger metasedimentary Neoproterozoic(?) crust to the east. The crust at the margin of the East Antarctic Craton may have been extended much later, possibly contributing to the observed weaker magnetic signatures.

8. Inferred extent of the Ferrar flood basalt province and sediment ages

Wilkes Basin magnetic anomalies are inferred to relate to Jurassic Ferrar rocks intruding Beacon Supergroup. This inference is justified by similarity with the magnetic anomalies and by seismic velocities over the adjacent Transantarctic Mountains [7,8]. Alternative interpretations such as relating them to Cenozoic basalts are less favoured. Previous radio-echo sounding sections reveal in fact subglacial mesa topography that may be attributed to Beacon Supergroup intruded by Ferrar sills across the Wilkes Basin [11]. The location of the Horn Bluff Ferrar outcrop along George V Coast (Fig. 1) is consistent with our magnetic interpretation for Ferrar tholeiites in the Wilkes Basin. Magnetic models at 78°S indicate that the Ferrar flood basalt province extends 250 km west of the Ross Sea rift margin [14]. Our magnetic data suggest that the Ferrar rocks continue into the Wilkes Basin. The Jurassic large igneous province at 75°S appears to be wider extending 400 km west of the Ross Sea rift margin. Contrary to previous assumptions the Ferrar Province is therefore not likely to be restricted to a narrow belt coinciding with the present-day Transantarctic Mountains.

Late Cretaceous and Cenozoic marine sedimentation in the Wilkes Basin region may be consistent with the occurrence of marine diatoms in the Sirius Group [32]. However, if sedimentary infill

of this age were several kilometres thick, then high-frequency magnetic anomalies would not have been observed over the Wilkes Basin, because the underlying Ferrar layer would be relatively deeper. Thick post-Jurassic rift infill may speculatively be possible in the 'Adventure Rift Basin' where Ferrar-type magnetic anomalies appear to be lacking. Thick Cenozoic(?) sedimentation in the rift basin may have occurred either prior to formation of the East Antarctic Ice Sheet(?) or during a low stand of the ice sheet [32]. Bright subglacial returns in radio-echo sounding data indicate that the 'Adventure Rift Basin' may contain water-saturated basal sediment [43]. Sedimentary rocks in moraines along the George V Coast strengthen the case for sedimentary sequences in the region [11].

9. Conclusions

ITASE potential field data combined with independent geophysical results hint at a more complex crustal structure than was previously suspected for the Wilkes Subglacial Basin region. Our potential field analysis provides new evidence for rifted crust at the East Antarctic Craton margin. The main results are summarised below.

1. Crustal thickness beneath the Wilkes Subglacial Basin is likely to be nearer 30 km at 75°S than the 45 km proposed from previous flexural modelling. Crustal thickness decreases from about 37 km beneath the Transantarctic Mountains to 31 ± 2 km under the broad 'Wilkes Extended Terrane', with a volcanosedimentary layer about 1–4 km thick. The narrower 'Adventure Rift Basin', by contrast, features a 25 ± 5 km thick crust and a 10 ± 4 km thick sedimentary infill.
2. The magnetic anomaly gradient at the western flank of the Wilkes Subglacial Basin may mark the eastern edge of the Precambrian East Antarctic Craton. The weakly magnetic Wilkes Subglacial Basin resembles the magnetic signature of the Neoproterozoic Adelaide fold belt of Australia. The subdued magnetic signature may also stem from much later broad crustal extension beneath the Wilkes Basin. A sharp aeromagnetic break may correspond to the eastern flank of the Wilkes Basin.
3. Magnetic and gravity anomalies over the Wilkes Subglacial Basin suggest the presence of Beacon Supergroup intruded by Jurassic rocks of the Ferrar Province. Thick Cenozoic(?) marine sedimentation in the 'Adventure Rift Basin' developed perhaps prior to the formation or during a low stand of the East Antarctic Ice sheet.

Acknowledgements

This research was supported by ENEA and the Università degli Studi di Milano and performed within the PNRA as part of the ITASE project. We thank members of the traverse team, personnel who assisted at the Terra Nova and Concordia Stations and those involved in traverse planning in Italy. G. Caneva gave technical advice. S. Urbini downloaded magnetic data. Scott Base and Terra Nova Bay magnetic observatories provided base station data. Two anonymous reviewers and Dr. Edward King performed detailed and constructive reviews of the manuscript.*[BW]*

References

[1] C.R. Bentley, Configuration and structure of the subglacial crust, in: R.J. Tingley (Ed.), The Geology of Antarctica, Oxford Monogr. Geol. Geophys., 14, Oxford University Press, New York, 1991, pp. 335–364.
[2] J.C. Behrendt, Crustal and lithospheric structure of the West Antarctic Rift System from geophysical investigations – a review, Global Planet. Change 23 (1999) 25–44.
[3] H. Trey, A.K. Cooper, G. Pellis, B. Della Vedova, G. Cochrane, G. Brancolini, J. Makris, Transect across the West Antarctic rift system in the Ross Sea, Antarctica, Tectonophysics 301 (1999) 61–74.
[4] K.H. Olsen, Continental Rifts: Evolution, Structure, Tectonics, Developments in Geotectonics 25, Elsevier, Amsterdam, 1995, 466 pp.
[5] G. Reitmayr, Gravity studies of Victoria Land and adjacent oceans, Antarctica, in: C.A. Ricci (Ed.), The Antarctic Region: Geological Evolution and Processes, Terra Antarctica, Siena, 1997, pp. 597–602.
[6] G. Reitmayr, V. Damm, E. Bozzo, G. Caneva, ACRUP Working Group, Gravity and ice thickness surveys along

ACRUP-1, in: C.A. Ricci (Ed.), The Antarctic Region: Geological Evolution and Processes, Terra Antarctica, Siena, 1997, pp. 619–626.
[7] F. Ferraccioli, E. Bozzo, Inherited crustal features and tectonic blocks of the Transantarctic Mountains: an aeromagnetic perspective (Victoria Land-Antarctica), J. Geophys. Res. 104 (1999) 25,297–25,319.
[8] B. Della Vedova, G. Pellis, H. Trey, J. Zhang, A.K. Cooper, J. Makris, ACRUP Working Group, Crustal structure of the Transantarctic Mountains, Western Ross Sea, in: C.A. Ricci (Ed.), The Antarctic Region: Geological Evolution and Processes, Terra Antarctica, Siena, 1997, pp. 609–618.
[9] D.J. Drewry, Sedimentary basins of the East Antarctic Craton from geophysical evidence, Tectonophysics 36 (1976) 301–314.
[10] D.J. Drewry, Antarctica: Glaciological and Geophysical Folio, Scott Polar Res. Inst., University Cambridge, Cambridge, 1983, 9 sheets.
[11] R.H.N Steed, Structural interpretation of Wilkes Land, Antarctica, in: R.L. Oliver, P.R. James, J.B. Jago (Eds.), Antarctic Earth Science-Proc. Fourth Int. Symp. Antarct. Earth Sci., Cambridge University Press, New York, 1983, pp. 567–572.
[12] T.A. Stern, U.S. ten Brink, Flexural uplift of the Transantarctic Mountains, J. Geophys. Res. 94 (1989) 10,315–10,330.
[13] U. ten Brink, T. Stern, Rift flank uplifts and hinterland basins: comparison of the Transantarctic Mountains with the Great Escarpment of Southern Africa, J. Geophys. Res. 97 (1992) 569–585.
[14] U.S. ten Brink, R.I. Hackney, S. Bannister, T.A. Stern, Y. Makovsky, Uplift of the Transantarctic Mountains and the bedrock beneath the East Antarctic ice sheet, J. Geophys. Res. 102 (B12) (1997) 27,603–27,621.
[15] M.B. Lythe, D.G. Vaughan, The BEDMAP Consortium, BEDMAP – bed topography of the Antarctic, 1:10,000,000 scale map, Cambridge, British Antarctic Survey (Misc) 9, 2000.
[16] A.P. Crary, Results of the United States Traverses in East Antarctica 1958–1961, IGY Glaciol. Rep., Am. Geogr. Soc. 7, 1963, 144 pp.
[17] E.S. Robinson, Geologic Structure of the Transantarctic Mountains and Adjacent Ice Covered Areas, Thesis, University of Wisconsin, Madison, WI, 1964, 290 pp.
[18] C.A. Ricci, F. Talarico, R. Palmeri, Tectonothermal evolution of the Antarctic Paleo-Pacific active margin of Gondwana: a northern Victoria Land perspective, in: C.A. Ricci (Ed.), The Antarctic Region: Geological Evolution and Processes, Terra Antarctica, Siena, 1997, pp. 591–596.
[19] S.G. Borg, D.J. De Paolo, Laurentia, Australia, and Antarctica as a Late Proterozoic supercontinent constraints from isotopic mapping, Geology 22 (1994) 307–310.
[20] R.L. Oliver, C.M. Fanning, Australia and Antarctica: precise correlation of Palaeoproterozoic Terrains, in: C.A. Ricci (Ed.), The Antarctic Region: Geological Evolution and Processes, Terra Antarctica, Siena, 1997, pp. 163–172.
[21] S.A. Ushakov, Some features of the structure of King George V Coast and Oates Coast according to geophysical data, Inf. Bull. Sov. Antarct. Exped. 18 (1960) 11–14.
[22] W. Bosum, D. Damaske, N.W. Roland, J.C. Behrendt, R. Saltus, The GANOVEX IV Victoria Land/Ross Sea aeromagnetic survey: interpretation of the anomalies, Geol. Jahrb. E38 (1989) 153–230.
[23] K.J. Woolfe, P.J. Barrett, Constraining the Devonian to Triassic tectonic evolution of the Ross Sea sector, Terra Antarct. 2 (1995) 7–21.
[24] J.W. Collinson, Paleoclimate of Permo-Triassic Antarctica, in: C.A. Ricci (Ed.), The Antarctic Region: Geological Evolution and Processes, Terra Antarctica, Siena, 1997, pp. 1029–1034.
[25] B.J. Encarnaciòn, T.H. Fleming, D.H. Elliot, H.V. Eales, Synchronous emplacement of Ferrar and Karoo dolerites and the early breakup of Gondwana, Geology 24 (1996) 535–538.
[26] T.J. Wilson, Jurassic faulting and magmatism in the Transantarctic Mountains: Implications for Gondwana breakup, in: R.H. Findlay, M.R. Banks, R. Unrug, J. Veevers, A.A. Balkema (Eds.), Gondwana 8 – Assembly, Evolution, and Dispersal, A.A. Balkema, Rotterdam, 1993, pp. 563–572.
[27] D.J. Schmidt, P.D. Rowley, Continental rifting and transform faulting along the Jurassic Transantarctic rift, Antarctica, Tectonics 5 (1986) 279–291.
[28] F.J. Davey, G. Brancolini, The Late Mesozoic and Cenozoic structural setting of the Ross Sea region, in: A.K. Cooper, P.F. Barker, G. Brancolini (Eds.), Geology and Seismic Stratigraphy of the Antarctic Margin, Antarct. Res. Ser., AGU 68 (1995) 167–182.
[29] F. Salvini, G. Brancolini, M. Busetti, F. Storti, F. Mazzarini, F. Coren, Cenozoic geodynamics of the Ross sea region, Antarctica: crustal extension, intraplate strike-slip faulting, and tectonic inheritance, J. Geophys. Res. 102 (B11) (1997) 24,669–24,696.
[30] T.J. Wilson, Cenozoic transtension along the Transantarctic Mountains-West Antarctic Rift boundary, southern Victoria Land, Antarctica, Tectonics 14 (1995) 531–545.
[31] Cape Roberts Science Team, Summary of results, in: P.J. Barrett, M. Sarti, W. Sherwood (Eds.), Initial Report on CRP-3, Terra Antarctica, Siena, 2000, pp. 185–209.
[32] P.N. Webb, D.M. Harwood, B.C. McKelvey, J.H. Mercer, L.D. Scott, Cenozoic marine sedimentation and ice-volume variation on the East Antarctic craton, Geology 12 (1984) 287–291.
[33] A.P. Stroeven, The Sirius Group of Antartica: age and environments, in: C.A. Ricci (Ed.), The Antarctic Region: Geological Evolution and Processes, Terra Antarctica, Siena, 1997, pp. 747–761.
[34] G. Cerrutti, F. Alasi, A. Germak, E. Bozzo, G. Caneva, R. Lanza, I. Marson, The absolute gravity station and the Mt. Melbourne gravity network in Terra Nova Bay,

North Victoria Land, East Antarctica, in: Y. Yoshida, K. Kaminuma, K. Shiraishi (Eds.), Recent Progress in Antarctic Earth Science, TERRAPUB, Tokyo, 1992, pp. 589–593.

[35] R.R.B. von Frese, L. Tan, J.W. Kim, C.R. Bentley, Antarctic crustal modeling from the spectral correlation of free-air gravity anomalies with the terrain, J. Geophys. Res. 104 (1999) 25,275–25,296.

[36] R.R.B. von Frese, H.R. Kim, L. Tan, J.W. Kim, P.T. Taylor, M.E. Purucker, D. Alsdorf, C.A. Raymond, Satellite magnetic anomalies of the Antarctic crust, Ann. Geofis. 42 (1999) 309–326.

[37] G. Dewart, M.N. Toksöz, Crustal structure in East Antarctica from surface wave dispersion, Geophys. J. 10 (1965) 127–139.

[38] A.A. Tikku, S.C. Cande, The oldest magnetic anomalies in the Australian-Antarctic Basin: are they isochrons?, J. Geophys. Res. 104 (1999) 661–677.

[39] M.E. Purucker, R.R.B. von Frese, P.T. Taylor, Mapping and interpretation of satellite magnetic anomalies from POGO data over the Antarctic region, Ann. Geofis. 42 (1999) 215–227.

[40] C. Tarlowski, P.R. Milligan, T. Mackey, Magnetic anomaly map of Australia (second edition): Australian Geological Survey Organisation, Canberra, 1996, scale 1:5 000 000.

[41] T. Flöttmann, P. James, J. Rogers, T. Johnson, Early Paleozoic foreland thrusting and basin reactivation at the Paleo-Pacific margin of the southeastern Australian Precambrian craton: a reappraisal of the structural evolution of the Southern Adelaide Fold-Thrust Belt, Tectonophysics 234 (1994) 95–116.

[42] F. Talarico, E. Armadillo, E. Bozzo, Antarctic rock magnetic properties: new susceptibility measurements in Oates Land and George V Land in the BACKTAM project, Terra Antarct. Rep. 5 (2000) 45–50.

[43] M.J. Seigert, J.K. Ridley, Determining basal ice-sheet conditions in the Dome C region of East Antarctica using satellite radar altimetry and airborne radio-echo sounding, J. Glac. 44 (1998) 1–8.